2026 IEEE International Conference on Robotics and Automation (ICRA 2026)
June 1-5, 2026. Vienna, Austria

PDLNet: Learning Point Cloud Distortion for Unsupervised Cross-domain Point Cloud Segmentation in Adverse Weather

Shuhua Dong[1], Minxian Li[1,2], Haofeng Zhang[1,2]

Abstract— **Existing point cloud semantic segmentation models are usually trained and evaluated using data collected under clear weather conditions. Under adverse weather conditions such as rain, snow and fog, point clouds are usually distorted and significant degradation of existing model performance occurs. Many domain adaptation methods try to address this issue by simulating adverse weather or using data augmentation techniques during training. However, they cannot accurately model the actual distortion in the target domain. By analyzing the visualization and statistical information of the target domain data and referring to existing studies, we categorize the distortion of point cloud data into position distortion, intensity distortion, and quantity distortion. To address these distortions of the target domain data, we propose a Point Distortion Learning Network (PDLNet) to integrate the Point Distortion Learning (PDL) module to learn the feature distortion of target domain data due to the adverse weather. Moreover, we also integrate the Cross-domain Feature Association (CFA) module to assist the model learn domain-invariant feature representations to improve the model's adaptability to the target domain. In addition, PDLNet introduces the Point Semantic Knowledge Distillation (PSKD) module, which ensures that only the target domain data is used efficiently in the inference phase while preserving the learned cross-domain knowledge. To further improve the model performance, we also iteratively optimize the model by introducing the curriculum learning module. Our approach establishes a new state-of-the-art level by achieving 40.6% mIoU and 27.7% mIoU in the SemanticKITTI-to-SemanticSTF and SynLiDAR-to-SemanticSTF benchmarks, respectively. Source code will be released at https://github.com/JerryD233/PDLNet.**

I. INTRODUCTION

Point cloud semantic segmentation is a fundamental task in the field of 3D computer vision, aiming to assign a category to each point in three-dimensional space. Point clouds are composed of a series of unordered data points distributed in three-dimensional space, typically obtained through LiDAR scanning. However, existing models for point cloud semantic segmentation are often trained and evaluated using data collected under clear weather conditions, showing significant performance degradation under adverse weather conditions such as rain, snow and fog.

The primary reason for this performance degradation is the distortion caused by adverse weather on LiDAR point cloud data. We visualized the point cloud data under clear weather (SemanticKITTI [1]) and adverse weather (SemanticSTF [2]), and performed statistical analysis on their intensity distributions, through which, with reference to existing studies, the distortion of point cloud data can be summarized into three aspects: (1) **Position Distortion**: Due to the refraction by droplets in the air and icy ground surfaces [3], [4], there is an offset in the coordinates of points. As shown in the Fig. 1(a), the positions of points are shifted under adverse weather conditions; (2) **Intensity Distortion**: Caused by scattering and energy absorption from droplets and snowflakes [5], [6], leading to changes in the reflection intensity of points in the point cloud data. As shown in the Fig. 1(b), the intensity distribution of road in adverse weather conditions is relatively unstable; (3) **Quantity Distortion**: Due to energy absorption by droplets and snowflakes [5], [4], [6], resulting in a reduction in the number of points in point cloud data. As shown in Fig. 1(c), adverse weather conditions can result in significant portions of the point cloud being missing.

In addition, obtaining point-wise annotations is costly, whereas unsupervised domain adaptation allows for the use of annotated source domain data and a small amount of unlabeled target domain data to train models and ensure high performance on the target domain. Therefore, we propose a Point Distortion Learning Network (PDLNet) to solve the point cloud data position and intensity distortions caused by bad weather. First, it standardizes, rescales and offsets voxel features in the source domain via the Point Distortion Learning (PDL) module to simulate position and intensity distortions in the target domain. Then, the Cross-domain Feature Association (CFA) module is proposed to establish the deep-level association between the features of the two domains through the cross-attention mechanism to realize adaptive feature matching and mitigate the feature distribution changes due to adverse weather. Finally, to avoid using the source data at the inference stage and lighten the inference network, the Point Semantic Knowledge Distillation (PSKD) module is introduced to use the inference results of the teacher model on the target domain as supervised information to train the student model directly on the target domain, with which the model can benefit from the cross-domain point semantic knowledge. All in all, our contributions are summarized as follows:

(1) Through the analysis of visualizations, statistical information and existing studies, we categorize the distortions of point cloud data caused by adverse weather into three types.

(2) In response to position and intensity distortions in point cloud data caused by adverse weather conditions, we propose the PDLNet, a method that can enhance the model's

[1]Nanjing University of Science and Technology. [2]State Key Laboratory of Intelligent Manufacturing of Advanced Construction Machinery. Correspondence to: Minxian Li <minxianli@njust.edu.cn>. This work was supported by the Key Research and Development Plan of Jiangsu Province (Industry Foresight and Key Core Technology Project) under Grant No. BE2023008-2.

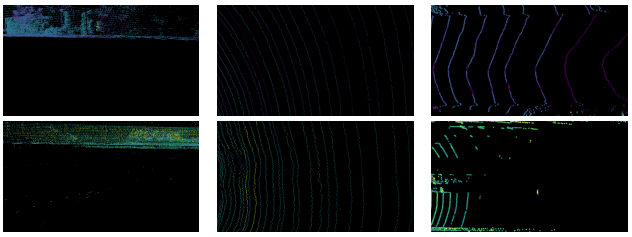

(a) Position Distortion (b) Intensity Distortion (c) Quantity Distortion

Fig. 1. Three Types of Point Cloud Distortion. The three images on the top are visualizations of LiDAR scans from SemanticKITTI [1] (clear weather), and the three images on the bottom are visualizations of LiDAR scans from SemanticSTF [2] (adverse weather). The intensity values are mapped to a color space with linearly increasing brightness, ranging from dark purple (low intensity) to bright yellow (high intensity).

adaptability to unseen adverse weather situations by learning the offsets of features caused by such weather conditions.

(3) Our method achieves state-of-the-art performance by improving 3.4% mIoU and 1.0% mIoU over the best existing UDA methods on the SemanticKITTI to SemanticSTF benchmark and SynLiDAR to SemanticSTF benchmark, respectively.

II. RELATED WORKS

A. Point Cloud Semantic Segmentation

Point cloud semantic segmentation aims to assign semantic labels to each point in a point cloud. In recent years, significant progress has been made in this field with the development of deep learning techniques. The existing methods can be mainly categorized into three types: (1) Point-based methods directly process raw point cloud data. Some studies [7], [8] use MLPs, others [9], [10] use CNNs, and still others [11] use transformers; (2) Projection-based methods project the 3D point cloud into a 2D representation. For example, some studies [12], [13] project the point cloud to range-view images, while others [14] project the point cloud to bird's-eye view; (3) Voxel-based methods represent point clouds as 3D voxels. Studies such as [15] use 3D dense convolutions, while [16], [17] use 3D sparse convolutions for processing efficiency.

B. UDA for Point Cloud Semantic Segmentation

Unsupervised Domain Adaptation (UDA) aims to solve the domain shift problem between source and target domains using source domain data and unlabeled target domain data. In point cloud semantic segmentation, some methods [13], [18] project point clouds to 2D images and use mature 2D UDA techniques for semantic segmentation. Other methods perform direct domain adaptation in 3D space by constructing intermediate domains [19], [20], domain mapping [21], [22], or domain mixing techniques [23]. Notably, UniMix [20] specifically targets adaptation from clear to adverse weather conditions by building a bridge domain through physical simulation of adverse weather and introducing universal mixing operations to fuse point cloud data from different domains. However, physical simulation cannot fully and accurately model the actual distortions in the target domain. Our method addresses the position and intensity distortions in point cloud data caused by adverse weather by directly simulating the feature shifts in target domain point clouds to reduce domain differences.

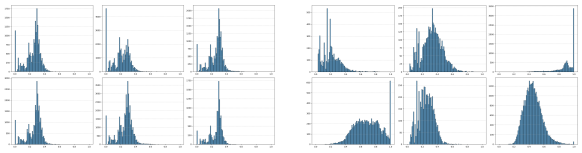

(a) Clear Weather (b) Adverse Weather

Fig. 2. Intensity Distribution Statistics of Road in Clear vs. Adverse Weather, the horizontal axis represents normalized intensity values, and the vertical axis represents the number of points. (a) We randomly selected 6 sequences from the training set of the SemanticKITTI [1] dataset, then randomly chose one frame from each sequence, the plot shows the statistical distribution of intensity values for points classified as road in these selected frames. (b) Similar to (a), but the data were statistically gathered from 6 randomly selected frames from the training set of the SemanticSTF [2] dataset.

C. 3D Scene Understanding in Adverse Weather

Due to the stringent safety requirements for outdoor navigation and perception tasks, 3D scene understanding under adverse weather has attracted increasing research attention in recent years. Previously, some works [3], [24], [25], [4] mainly explored methods for 3D object detection under adverse weather conditions such as rain, snow and fog. The STF [26] is a large-scale multimodal dataset for 3D object detection in adverse weather conditions. SemanticSTF [2] extends STF [26] by adding semantic labels, upon which several works [27], [28], [29], [20] have explored methods for 3D semantic segmentation under adverse weather conditions.

III. METHOD

A. Problem Definition

In the task of UDA point cloud semantic segmentation for adverse weather, we aim to solve the domain shift problem between the source domain (clear weather conditions) and the target domain (adverse weather conditions such as rain, snow, fog, etc.) in order to improve the segmentation model's generalization performance in unseen scenes under adverse weather conditions. Let us define the source domain and the target domain as follows:

The source domain data can be represented as a point cloud set $\mathcal{X}_s = \{(x_s^i, y_s^i)\}_{i=1}^m$, where x_s^i denotes 3D point cloud data under clear weather conditions, y_s^i represents the point-wise annotated semantic labels, and m indicates the total number of source domain samples. The target domain data is represented as an unlabeled point cloud set $\mathcal{X}_t = \{x_t^j\}_{j=1}^n$, where x_t^j corresponds to 3D point cloud data collected under adverse weather conditions, with n being the total number of target domain samples.

B. Point Cloud Distortion

Adverse weather can cause distortions in point cloud data, which we categorize into three types:

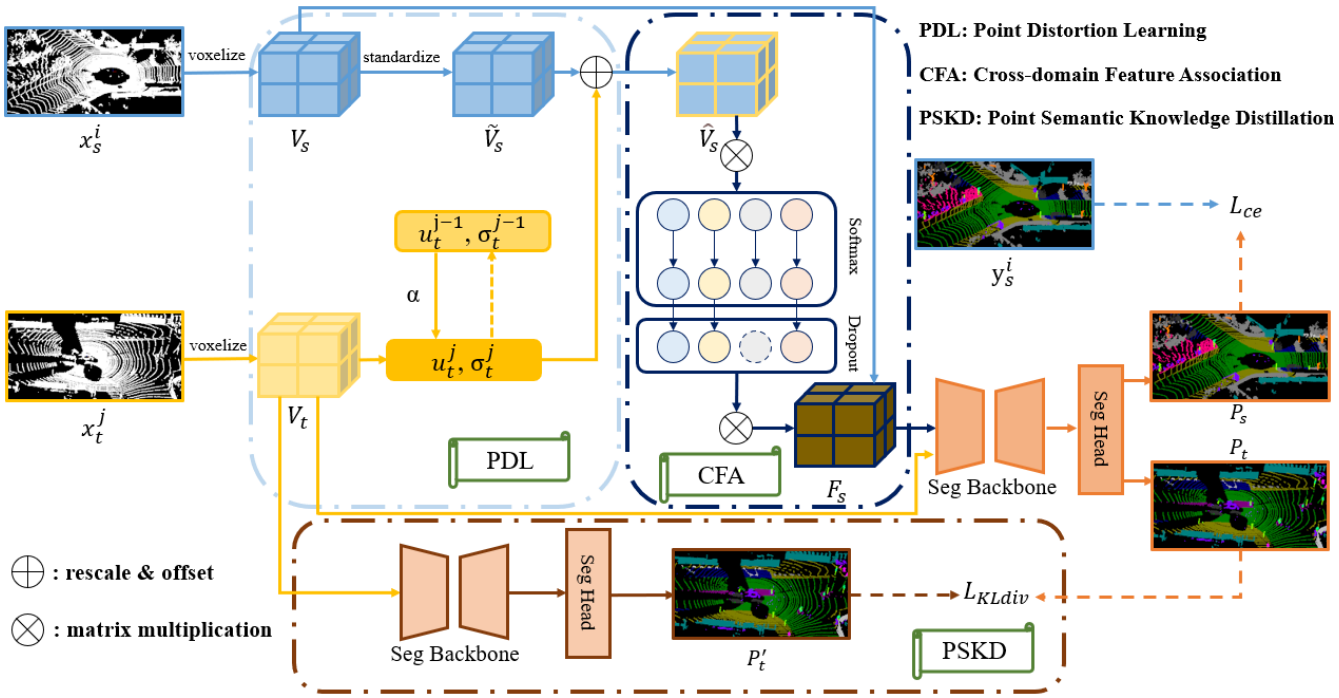

Fig. 3. Illustration of the PDLNet Architecture. First, the source and target domain point clouds are voxelized to obtain voxel features respectively, and then the feature shift of the target domain point cloud due to adverse weather is migrated to the source domain by the Point Distortion Learning (PDL) module, after which the domain-invariant feature representations are obtained by the Cross-domain Feature Association (CFA) module, and finally the point semantic knowledge learned from the teacher's network is distilled to the student's network by the Point Semantic Knowledge Distillation (PSKD) module. Where the blue lines represent the source part, the gold lines stand for the target domain part, the light blue lines are for the PDL module, the dark blue lines represent the CFA module, the dark orange lines correspond to the KT module, and the orange line represent the semantic segmentation part.

(1) **Position Distortion:** This phenomenon mainly results from the refraction and reflection of laser beams by atmospheric particles (e.g., raindrops, snowflakes, fog) and reflective ground surfaces such as ice or water [3], [4]. These factors alter the LiDAR signal path, causing inaccuracies in 3D point coordinates. Points collected in adverse weather show more significant jitter and spatial inconsistency than those captured in clear conditions. As shown in Fig. 1(a), we visualize the data from clear weather (top) and adverse weather (bottom), respectively. It can be clearly observed that the certain points corresponding to road exhibit significant positional displacement under adverse weather.

(2) **Intensity Distortion:** Intensity values represent the reflectivity of the scanned surface and are crucial for semantic segmentation task. However, these values are heavily affected by scattering and partial energy absorption caused by airborne particles such as water droplets and snowflakes [5], [6]. As illustrated in Fig. 1(b), while the intensity distribution of road surfaces remains relatively stable in clear weather data, it becomes highly variable under adverse weather conditions. Additionally, we randomly selected multiple scans under both clear and adverse weather for each category and statistically analyzed the intensity value distributions. The results show that the distribution of intensity values of road in clear weather data remains relatively stable, while in adverse weather, the distribution of intensity values of road in different frames changes significantly, which may be due to changes in the type and severity of weather (such as heavy rain versus light rain). To better show the intensity distribution variations, we visualize 6 randomly selected frames from the statistics for the road categories with the highest frequency of occurrence, which can be seen in Fig. 2.

(3) **Quantity Distortion:** Signal attenuation occurs as LiDAR pulses pass through dense particles such as water droplets and snowflakes, which absorb or scatter the beam before it reaches the target [5], [4], [6]. This leads to missing echoes and incomplete point cloud data. As shown in Fig. 1(c), some portions of the scene, especially distant areas, significantly miss in the adverse weather scans. In addition, we also counted the average number of point clouds per frame in training set for sunny day and severe weather data separately. The clear weather data have an average of about 122,820 points per frame, while the adverse has only an average of about 47,812 points per frame, which indicates that adverse weather can cause a significant decrease in the number of points.

To address the position distortion and intensity distortion in point cloud data caused by adverse weather conditions, we use labeled source domain data $\mathcal{X}_s$ and unlabeled target domain data $\mathcal{X}_t$ to simulate the offsets of point position features and changes of intensity features in the target domain, training a segmentation model that can effectively perform segmentation tasks on the target domain $\mathcal{X}_t$.

C. Overall Architecture

The overall architecture of the proposed PDLNet is shown in Fig. 3. First, we voxelize the source-domain point cloud x_s^i and the target-domain point cloud x_t^j to obtain the voxel features V_s and V_t, respectively. Then, we improve the AdaIN [30] and design the Point Distortion Learning (PDL) module based on it to migrate the target-domain feature shifts caused by severe weather to the source-domain data by standardizing, rescaling and offsetting the source-domain features to simulate the position distortion and intensity distortion of the target-domain point cloud data.

Second, we design the Cross-domain Feature Association (CFA) module to learn inter-domain invariant feature representations. This module establishes deep associations between source domain features and target domain features through the cross-attention mechanism. Specifically, it takes the source domain feature $\widehat{V}_s$ processed by the PDL module as the query and the target domain feature V_t as the key and value, and realizes the inter-domain adaptive feature matching through the attentional weight computation, which effectively mitigates the feature distribution shift caused by the adverse weather.

Finally, considering the impracticality of using source domain data in the inference process, we introduce the Point Semantic Knowledge Distillation (PSKD) module. This module employs the teacher model's inference results on the target domain as supervision and uses target domain data as training data to train a student model. Such design not only allows for directly training the model on unlabeled target domain data but also enables the model to benefit from the cross-domain point semantic knowledge learned by the teacher model.

D. Point Distortion Learning

In unsupervised domain adaptation for point cloud semantic segmentation under adverse weather conditions, the target domain point clouds exhibit position and intensity distortions due to inclement weather, manifesting as coordinate shifts and intensity variations. Therefore, this paper design the Point Distortion Learning module to migrate the feature shift of the target-domain point cloud data due to adverse weather to the source-domain data. This module adopts the idea of AdaIN [30], which, however, is only suitable for the transfer of single sample pairs. To address dataset-level transfer, we extract global statistics to facilitate the adaptation across datasets.

First, we voxelize source domain point clouds x_s^i and target domain point clouds x_t^j to obtain voxel features V_s and V_t respectively. Then, we standardize V_s, using the following formula:

$$\tilde{V}_s = \frac{V_s - E(V_s)}{\sqrt{D(V_s)}}, \tag{1}$$

where $\tilde{V}_s$ is the standardized V_s, and $E(\cdot)$ and $D(\cdot)$ represent the operations for calculating the mean and variance, respectively.

Subsequently, we compute the statistics of the target domain features to extract the feature offsets in the target domain due to adverse weather. Specifically, instead of extracting for a single sample, we extract the global feature offsets. The μ_t^j and σ_t^j of the target domain data at the j-th iteration are obtained by the following formulas:

$$\begin{cases} \mu_t^j = (1-\alpha)\cdot \mu_t^{j-1} + \alpha \cdot \sqrt{D(V_t)} \\ \sigma_t^j = (1-\alpha)\cdot \sigma_t^{j-1} + \alpha \cdot E(V_t) \end{cases}, \tag{2}$$

where $j \in \mathbb{Z}$ and $j > 0$, additionally we let $\mu_t^0 = \mu_t^1$ and $\sigma_t^0 = \sigma_t^1$. Since the amount of target domain data is much smaller compared to the source domain, during the early stages of one training epoch, μ_t^j and σ_t^j can respectively represent the global mean and global standard deviation.

Subsequently, we use the statistics of the target domain features to rescale and offset the source domain features to obtain the weather-affected source domain features $\hat{V}_s$. The specific formulas are as follows:

$$\hat{V}_s = \sigma_t^j \cdot \tilde{V}_s + \mu_t^j. \tag{3}$$

E. Cross-domain Feature Association

In order to achieve effective cross-domain feature associations and thus obtain domain-invariant feature representations to improve the generalization performance of the model, we utilize the cross-attention mechanism by treating source domain data as the query and target domain data as the key and value. With this approach, we can capture fine-grained interactions between features from different domains. It is worth noting that GPU memory is prone to overflow when applying the cross-attention mechanism to voxel features, so we adopt a chunked computation approach.

First, the attention-weighted feature A_l for the l-th chunk is computed as:

$$A_l = \gamma\left(\delta\left(\frac{(w_q\hat{V}_{s,l})(w_kV_t)^T}{\sqrt{d}}\right)\right)\cdot(w_vV_t), \tag{4}$$

where w_q, w_k, and w_v represent the weights for the query, key and value matrices respectively, d is the dimension of the key vectors, $\hat{V}_{s,l}$ denotes the l-th chunk of $\hat{V}_s$, $\delta(\cdot)$ refers to the softmax function, $\gamma(\cdot)$ refers to the dropout function.

Then, the cross-domain enhanced feature F_s is obtained as follows:

$$F_s = \text{Concat}\left(\{A_l\}_{l=0}^{\lceil e/L\rceil-1}\right) + V_s, \tag{5}$$

where e is the length of $\hat{V}_s$, L represents the predefined chunk size, and Concat$(\cdot)$ indicates concatenation along a specific dimension.

After the above processing we get the initial feature F_s, which is fed into the backbone network for semantic segmentation of the point cloud and a segmentation header is used to get the predicted probability P_s and P_t. Finally, we employ the standard cross-entropy loss L_{ce} [31] to supervise the predictions on the source domain.

F. Point Semantic Knowledge Distillation

Considering that we should not have access to the source domain data during the inference phase, we use the Point Semantic Knowledge Distillation module to achieve direct training on the target domain, employing the teacher model's predicted probability P_t on the target domain as the supervision in order to fully transfer the cross-domain point semantic knowledge learned by the full model to the student model, which only needs the target domain data. In addition, we use the Kullback-Leibler (KL) divergence as the supervised loss during the training of the student model, denoted as L_{KL}. Therefore, the overall loss L_{seg} for network training is given by:

$$L_{seg} = L_{ce}(P_s, y_s) + \lambda L_{KL}(P'_t, P_t), \tag{6}$$

where P_s is the predicted probability of teacher model on source domain, y_s is the semantic GT on source domain, P'_t is the predicted probability of student model on target domain, P_t is the predicted probability of teacher model on target domain, and λ is a balancing coefficient.

G. Curriculum Learning

Curriculum learning has been proven its effectiveness by previous studies [32], [33]. Therefore, after the first training phase of PDLNet, we introduced the Curriculum Learning (CL) module to improve the performance of the model in the target domain. Specifically, we use the inference results of the student model in the target domain obtained from the first stage of training as the initial supervision for the second stage of training. Thereafter we use the predictions of the model obtained from the previous epoch of training as the new pseudo-labels for current epoch. For selecting the high-confidence pseudo-label, we design a confidence condition function to eliminate the low quality predictions from the previous epoch.

In the k-th training epoch, given the predicted semantic probability distribution $P'_t(q)$ of the point q, the pseudo-label $y'_t(q)$ can be computed as follows:

$$y'_t(q) = \arg\max_c \left(P'_t(q)\right) \cdot \mathbf{I}\left(P'_t(q) > (\epsilon_0 - \Delta\epsilon \cdot k) \cdot M(c)\right), \tag{7}$$

where c is the model's classification result for point q, $\epsilon_0 - \Delta\epsilon \cdot k$ represents the threshold, and $\epsilon_0 - \Delta\epsilon \cdot k \geq 0$, ϵ_0 is a scalar, $\Delta\epsilon$ is the reduction amount, $\mathbf{I}(\cdot)$ is an indicator function that equals 1 when the condition is met and 0 otherwise, $M(c)$ denotes the maximum probability that the point predicted by the model in the current LiDAR frame belongs to category c. Subsequently the selected pseudo-label $y'_t(q)$ are used as supervised signal for $(k+1)$-th training epoch with cross-entropy loss.

IV. Experiments

A. Datasets and Metrics

1) Datasets.: We utilize synthetic datasets SemanticKITTI [1] and SyLiDAR [22] as our source domains, and the adverse-weather SemanticSTF dataset [2] as our target domain for experimental evaluation.

SemanticKITTI [1] is a real-world LiDAR dataset extending the KITTI Vision Benchmark [34], providing dense point-wise annotations for 28 semantic categories across diverse urban and rural scenes. We adopt the official split, using sequences 00–07 and 09–10 (19,130 scans) for training and sequence 08 (4,071 scans) for validation. **SynLiDAR** [22] is a synthetic LiDAR dataset generated via Unreal Engine 4, which provides accurate point-wise annotations for 32 semantic categories in simulated urban, suburban, and harbor environments. Following the common practice [27], [28], [29], [20], we use 19,840 scans for training and 1,976 for validation. **SemanticSTF** [2] is an adverse-weather LiDAR dataset derived from the STF benchmark [26], offering point-wise annotations for 21 semantic categories across diverse weather conditions, including 637 dense fog, 631 light fog, 114 rain, and 694 snow scenes. We adhere to the official split, utilizing 1,326 scans for training and 250 scans for validation.

2) Metrics.: For performance evaluation, we employ two standard metrics: class-wise Intersection over Union (IoU) and mean IoU (mIoU) across all categories. To ensure fair comparison across domains, we unify the label spaces by mapping all datasets (SemanticKITTI [1], SynLiDAR [22], and SemanticSTF [2]) to the 19 common semantic classes defined in SemanticKITTI, following established practices in cross-domain segmentation [20].

B. Experimental Settings

In PDLNet, we utilize MinkowskiNet [16] as the backbone network for point cloud semantic segmentation. The model is trained using the Stochastic Gradient Descent (SGD) algorithm with a momentum parameter set to 0.9. Initially, the learning rate is configured to 0.24 and progressively diminishes as the number of training epochs increases. Our training is divided into two stages, in the first stage, we train the teacher and student models simultaneously, as shown in Fig. 3, for a total of 15 epochs; in the second stage, we use curriculum learning for training, for a total of 30 epochs. The complete training procedure requires approximately 25 hours when executed on four RTX 3090 GPUs. For each experiment, we set $\alpha = 0.1$ in cEq. (2). The loss weight λ in Eq. (6) is set to 1. Additionally, we set $\epsilon_0 = 0.9$ and $\Delta\epsilon = 0.1$ in Eq. (7) in curriculum learning.

C. Main Results

1) SemanticKITTI to SemanticSTF.: As shown in the top part of Table I, we use SemanticKITTI as the source domain and SemanticSTF with all four weather conditions as the target, and our PDLNet achieves state-of-the-art performance of 40.6% mIoU, which is an improvement of 16.2% mIoU over the source-only model, and an improvement of 3.4% mIoU over the current best method UniMix [20] (37.2% mIoU). In addition, we train a separate model for each specific weather subset of SemanticSTF, which are trained using only the corresponding specific weather data, and evaluate the trained models against the trained weather conditions. From Table II,

TABLE I

COMPARISON OF SOTA DOMAIN ADAPTATION METHODS ON SEMANTICKITTI→SEMANTICSTF AND SYNLIDAR→SEMANTICSTF.

Method	car	bi.cle	mt.cle	truck	oth-v.	pers.	bi.clst	mt.clst	road	parki.	sidew.	oth-g.	build.	fence	veget.	trunk	terra.	pole	traf.	mIoU
Oracle	89.4	42.1	0.0	59.9	61.2	69.6	39.0	0.0	82.2	21.5	58.2	45.6	86.1	63.6	80.2	52.0	77.6	50.1	61.7	54.7
SemanticKITTI→SemanticSTF																				
Source-only	55.9	0.0	0.2	1.9	10.9	10.3	6.0	0.0	61.2	10.9	32.0	0.0	67.9	41.6	49.8	27.9	40.8	29.6	17.5	24.4
ADDA [35]	65.6	0.0	0.0	21.0	1.3	2.8	1.3	16.7	64.7	1.2	35.4	0.0	66.5	41.8	57.2	32.6	42.2	23.3	26.4	26.3
Ent-Min [36]	69.2	0.0	10.1	31.0	5.3	2.8	2.6	0.0	65.9	2.6	35.7	0.0	72.5	42.8	52.4	32.5	44.7	24.7	21.1	27.2
Self-training [37]	71.5	0.0	10.3	**33.1**	7.4	5.9	1.3	0.0	65.1	6.5	36.6	0.0	67.8	41.3	51.7	32.9	42.9	25.1	25.0	27.6
CoSMix [23]	65.0	**1.7**	22.1	25.2	7.7	33.2	0.0	0.0	64.7	11.5	31.1	0.9	62.5	37.8	44.6	30.5	41.1	30.9	28.6	28.4
UniMix [20]	75.3	0.9	**44.9**	11.7	**13.6**	38.2	**50.3**	**31.9**	71.1	**15.0**	46.4	6.5	74.3	51.0	49.8	36.8	34.4	25.5	28.9	37.2
PDLNet	**84.3**	0.9	0.0	31.3	12.7	**54.1**	0.0	0.0	**77.7**	7.2	**52.0**	**34.0**	**82.0**	**58.4**	**76.2**	**43.5**	**69.6**	**39.5**	**48.8**	**40.6**
SynLiDAR→SemanticSTF																				
Source-only	27.1	**3.0**	0.6	15.8	0.1	25.2	1.8	5.6	23.9	0.3	14.6	0.6	36.3	19.9	37.9	17.9	41.8	9.5	2.3	15.0
ADDA [35]	55.8	0.0	3.6	26.1	1.3	25.2	7.5	9.9	17.2	**23.4**	4.4	0.9	43.9	18.4	45.2	21.8	33.6	28.0	19.7	20.3
Ent-Min [36]	48.3	0.1	5.6	28.7	0.1	23.3	2.5	19.8	19.3	6.7	22.6	1.4	46.9	20.7	43.2	25.2	34.1	26.0	22.2	20.9
Self-training [37]	50.6	0.0	6.1	**31.0**	0.5	26.0	4.8	12.0	20.7	4.6	23.5	1.5	45.3	19.5	44.6	25.0	35.1	**29.2**	20.8	21.1
CoSMix [23]	51.5	0.2	5.0	28.1	0.0	26.5	**17.0**	9.9	20.2	3.6	24.6	2.2	52.6	20.6	47.5	24.3	34.6	28.2	24.1	22.1
UniMix [20]	73.6	0.0	**7.9**	26.9	**2.9**	**29.1**	13.7	**21.8**	**38.0**	8.0	26.3	3.4	56.0	21.2	56.1	**29.6**	38.0	28.2	**26.5**	26.7
PDLNet	**72.6**	0.0	0.0	12.5	0.0	16.1	0.0	0.0	71.4	1.3	**38.7**	**20.6**	**70.2**	**47.8**	**63.8**	8.6	**60.4**	27.7	14.5	**27.7**

we can learn that our method works better than all existing methods.

2) SynLiDAR to SemanticSTF: As shown in the bottom half of Table I, in terms of synthetic-to-real adaptation (SynLiDAR→SemanticSTF), PDLNet refreshes the state-of-the-art with 26.7% mIoU, which is an improvement of 12.7% mIoU over the source-only model (15.0% mIoU), and 1.0% mIoU over UniMix [20] (26.7% mIoU). In addition, PDLNet achieves a performance gap of 12.9% mIoU between the SemanticKITTI→SemanticSTF scenario and the SynLiDAR→SemanticSTF scenario, which could be attributed to the additional domain shift encountered when transitioning from a synthetic dataset to a real-world dataset [20].

D. Ablation Studies

As shown in Table III, we performed ablation experiments on our method, and in the following we analyze the effectiveness of each module we used.

Efficacy of the PDL module. By introducing PDL, we observed that the mIoU on the SemanticKITTI dataset increased from 24.4% (Source-only) to 35.3%, and on the SynLiDAR dataset from 15.0% to 19.3%. This indicates that PDL enables the source domain point cloud data to effectively simulate the feature shifts of the target domain point cloud data due to adverse weather, which improves the generalization ability of the model.

Efficacy of the CFA module. Further integrating CFA led to an mIoU of 37.4% on the SemanticKITTI dataset, a significant improvement over using PDL alone. On the SynLiDAR dataset, the mIoU also improved from 21.4% to 22.6%. This suggests that CFA, by correlating cross-domain features, can enable the model to effectively learn domain-invariant feature representations in order to further enhance the generalization ability of the model.

Efficacy of the PSKD module. Source domain data is not supposed to be used in the inference phase, and the PSKD module, which allows the analysis of target domain data only, is important for PDLNet. After the introduction of the PSKD module, the mIoU of the SemanticKITTI dataset reached 35.7% from 37.4%, and that of the SynLiDAR dataset increased from 22.6% to 26.9%, indicating that the Point Semantic Knowledge Distillation module not only allows the inference network to be lightweight, but also improves the performance of the model.

Efficacy of the CL module. After further employing the CL technique, the mIoU reaches 40.6% for the SemanticKITTI dataset and 27.7% for the SynLiDAR dataset, which is an increase of 1.4% and 0.8%, respectively, compared to the no-CL technique. These results indicate that the Curriculum learning technique contributes to the performance of model. In addition, we analyze $\Delta\epsilon$, Table IV shows that 0.1 is the best choice.

V. CONCLUSION

In this paper, we categorize the distortion of point cloud data due to severe weather into position distortion, intensity distortion, and quantitative distortion, and propose PDLNet, a UDA framework that can improve the model's adaptability to unknown severe weather conditions, for position distortion and intensity distortion. In the PDL module, after normalizing the source-domain voxel features, we simulate the feature shifts occurring in the point cloud due to severe weather by rescaling and shifting the source-domain voxel features using

TABLE II

COMPARISON OF STATE-OF-THE-ART DOMAIN ADAPTATION METHODS ON SEMANTICKITTI→SEMANTICSTF ADAPTATION FOR INDIVIDUAL ADVERSE WEATHER CONDITIONS.

Method	Dense-fog	Light-fog	Rain	Snow
Source-Only	26.9	25.2	27.7	23.5
ADDA [35]	31.5	27.9	27.4	23.4
Ent-Min [36]	31.4	28.6	30.3	24.9
Self-training [37]	31.8	29.3	27.9	25.1
CoSMix [23]	31.6	30.3	33.1	32.9
UniMix [20]	40.0	32.0	39.3	31.6
PDLNet	**40.9**	**40.3**	**46.3**	**39.9**

TABLE III

ABLATION STUDY OF PDLNET ON SEMANTICKITTI→SEMANTICSTF AND SYNLIDAR→SEMANTICSTF.

Method	car	bi.cle	mt.cle	truck	oth-v.	pers.	bi.clst	mt.clst	road	parki.	sidew.	oth-g.	build.	fence	veget.	trunk	terra.	pole	traf.	mIoU
SemanticKITTI→SemanticSTF																				
Source-only	55.9	0.0	0.2	1.9	10.9	10.3	6.0	0.0	61.2	10.9	32.0	0.0	67.9	41.6	49.8	27.9	40.8	29.6	17.5	24.4
+PDL	81.0	0.6	12.9	40.3	19.0	42.3	7.1	25.3	60.3	13.8	34.7	5.2	74.9	45.8	59.1	36.5	46.9	28.8	36.4	35.3
+CFA	81.5	1.0	23.8	42.5	23.9	41.8	5.6	45.7	57.0	13.6	36.0	4.0	75.7	48.3	60.5	33.9	49.8	27.9	38.1	37.4
+PSKD	82.7	0.0	52.0	45.4	27.8	44.7	1.0	0.0	68.4	8.6	42.7	5.1	79.7	53.9	57.3	38.2	49.4	29.7	39.6	38.2
+CL	84.3	0.9	0.0	31.3	12.7	54.1	0.0	0.0	77.7	7.2	52.0	34.0	82.0	58.4	76.2	43.5	69.6	39.5	48.8	40.6
SynLiDAR→SemanticSTF																				
Source-only	27.1	3.0	0.6	15.8	0.1	25.2	1.8	5.6	23.9	0.3	14.6	0.6	36.3	19.9	37.9	17.9	41.8	9.5	2.3	15.0
+PDL	55.4	6.3	3.1	20.5	2.8	29.9	2.7	4.8	50.4	4.8	22.3	0.0	53.7	15.4	47.1	25.6	38.1	18.0	5.9	21.4
+CFA	64.0	3.5	2.3	23.3	4.4	26.1	1.6	4.6	47.4	3.1	21.9	0.0	53.9	27.8	50.0	22.6	42.4	22.8	7.7	22.6
+PSKD	75.8	3.5	4.9	36.3	0.1	42.8	4.7	8.3	62.1	0.0	27.5	0.0	63.0	31.3	53.6	23.8	32.4	30.9	10.5	26.9
+CL	72.6	0.0	0.0	12.5	0.0	16.1	0.0	0.0	71.4	1.3	38.7	20.6	70.2	47.8	63.8	8.6	60.4	27.7	14.5	27.7

TABLE IV

CL PERFORMANCE ON SEMANTICKITTI→SEMANTICSTF WITH VARIOUS $\Delta\epsilon$.

$\Delta\epsilon$	car	bi.cle	mt.cle	truck	oth-v.	pers.	bi.clst	mt.clst	road	parki.	sidew.	oth-g.	build.	fence	veget.	trunk	terra.	pole	traf.	mIoU
0.08	84.1	0.9	0.0	31.1	12.7	54.4	0.0	0.0	77.3	5.6	51.8	33.5	82.0	57.9	76.1	43.6	69.1	39.0	48.5	40.4
0.1	84.3	0.9	0.0	31.3	12.7	54.1	0.0	0.0	77.7	7.2	52.0	34.0	82.0	58.4	76.2	43.5	69.6	39.5	48.8	40.6
0.12	84.0	2.2	0.0	28.5	9.4	52.9	0.0	0.0	77.3	4.7	51.5	32.7	80.3	56.1	75.9	42.4	69.0	38.6	47.5	39.7

the extracted statistical information of the target domain. In addition, we further utilize the CFA module to allow the model to learn the cross-domain invariant feature representation, which improves the model's adaptability to the target domain. We conducted experiments on two benchmarks to prove the effectiveness of our method and designed ablation experiments to demonstrate the effectiveness of each module in our method.

REFERENCES

[1] J. Behley, M. Garbade, A. Milioto, J. Quenzel, S. Behnke, C. Stachniss, and J. Gall, "Semantickitti: A dataset for semantic scene understanding of lidar sequences," in *ICCV*, 2019, pp. 9297–9307.

[2] A. Xiao, J. Huang, W. Xuan, R. Ren, K. Liu, D. Guan, A. El Saddik, S. Lu, and E. P. Xing, "3d semantic segmentation in the wild: Learning generalized models for adverse-condition point clouds," in *CVPR*, 2023, pp. 9382–9392.

[3] M. Hahner, C. Sakaridis, M. Bijelic, F. Heide, F. Yu, D. Dai, and L. Van Gool, "Lidar snowfall simulation for robust 3d object detection," in *CVPR*, 2022, pp. 16 364–16 374.

[4] V. Kilic, D. Hegde, A. B. Cooper, V. M. Patel, and M. Foster, "Lidar light scattering augmentation (lisa): Physics-based simulation of adverse weather conditions for 3d object detection," in *ICASSP*, 2025, pp. 1–5.

[5] T. Fersch, A. Buhmann, A. Koelpin, and R. Weigel, "The influence of rain on small aperture lidar sensors," in *GeMiC*, 2016, pp. 84–87.

[6] J. Shin, H. Park, and T. Kim, "Characteristics of laser backscattering intensity to detect frozen and wet surfaces on roads," *J Sensors*, vol. 2019, no. 1, p. 8973248, 2019.

[7] C. R. Qi, L. Yi, H. Su, and L. J. Guibas, "Pointnet++: Deep hierarchical feature learning on point sets in a metric space," *NeurIPS*, vol. 30, 2017.

[8] H. Zhao, L. Jiang, C.-W. Fu, and J. Jia, "Pointweb: Enhancing local neighborhood features for point cloud processing," in *CVPR*, 2019, pp. 5565–5573.

[9] Y. Li, R. Bu, M. Sun, W. Wu, X. Di, and B. Chen, "Pointcnn: Convolution on x-transformed points," in *NeurIPS*, vol. 31, 2018.

[10] W. Wu, Z. Qi, and L. Fuxin, "Pointconv: Deep convolutional networks on 3d point clouds," in *CVPR*, 2019, pp. 9621–9630.

[11] L. Duan, S. Zhao, N. Xue, M. Gong, G.-S. Xia, and D. Tao, "Condaformer: Disassembled transformer with local structure enhancement for 3d point cloud understanding," in *NeurIPS*, vol. 36, 2023, pp. 23 886–23 901.

[12] B. Wu, A. Wan, X. Yue, and K. Keutzer, "Squeezeseg: Convolutional neural nets with recurrent crf for real-time road-object segmentation from 3d lidar point cloud," in *ICRA*, 2018, pp. 1887–1893.

[13] B. Wu, X. Zhou, S. Zhao, X. Yue, and K. Keutzer, "Squeezesegv2: Improved model structure and unsupervised domain adaptation for road-object segmentation from a lidar point cloud," in *ICRA*, 2019, pp. 4376–4382.

[14] Y. Zhang, Z. Zhou, P. David, X. Yue, Z. Xi, B. Gong, and H. Foroosh, "Polarnet: An improved grid representation for online lidar point clouds semantic segmentation," in *CVPR*, 2020, pp. 9601–9610.

[15] Z. Wu, S. Song, A. Khosla, F. Yu, L. Zhang, X. Tang, and J. Xiao, "3d shapenets: A deep representation for volumetric shapes," in *CVPR*, 2015, pp. 1912–1920.

[16] C. Choy, J. Gwak, and S. Savarese, "4d spatio-temporal convnets: Minkowski convolutional neural networks," in *CVPR*, 2019, pp. 3075–3084.

[17] B. Graham, M. Engelcke, and L. Van Der Maaten, "3d semantic segmentation with submanifold sparse convolutional networks," in *CVPR*, 2018, pp. 9224–9232.

[18] S. Zhao, Y. Wang, B. Li, B. Wu, Y. Gao, P. Xu, T. Darrell, and K. Keutzer, "epointda: An end-to-end simulation-to-real domain adaptation framework for lidar point cloud segmentation," in *AAAI*, vol. 35, 2021, pp. 3500–3509.

[19] L. Yi, B. Gong, and T. Funkhouser, "Complete & label: A domain adaptation approach to semantic segmentation of lidar point clouds," in *CVPR*, 2021, pp. 15 363–15 373.

[20] H. Zhao, J. Zhang, Z. Chen, S. Zhao, and D. Tao, "Unimix: Towards domain adaptive and generalizable lidar semantic segmentation in adverse weather," in *CVPR*, 2024, pp. 14 781–14 791.

[21] F. Langer, A. Milioto, A. Haag, J. Behley, and C. Stachniss, "Domain transfer for semantic segmentation of lidar data using deep neural networks," in *IROS*, 2020, pp. 8263–8270.

[22] A. Xiao, J. Huang, D. Guan, F. Zhan, and S. Lu, "Transfer learning from synthetic to real lidar point cloud for semantic segmentation," in *AAAI*, vol. 36, 2022, pp. 2795–2803.

[23] C. Saltori, F. Galasso, G. Fiameni, N. Sebe, F. Poiesi, and E. Ricci, "Compositional semantic mix for domain adaptation in point cloud segmentation," *IEEE TPAMI*, vol. 45, no. 12, pp. 14 234–14 247, 2023.

[24] M. Hahner, C. Sakaridis, D. Dai, and L. Van Gool, "Fog simulation on real lidar point clouds for 3d object detection in adverse weather," in *ICCV*, 2021, pp. 15 283–15 292.

[25] X. Huang, H. Wu, X. Li, X. Fan, C. Wen, and C. Wang, "Sunshine to rainstorm: Cross-weather knowledge distillation for robust 3d object detection," in *AAAI*, vol. 38, 2024, pp. 2409–2416.

[26] M. Bijelic, T. Gruber, F. Mannan, F. Kraus, W. Ritter, K. Dietmayer, and F. Heide, "Seeing through fog without seeing fog: Deep multimodal sensor fusion in unseen adverse weather," in *CVPR*, 2020, pp. 11 682–11 692.

[27] J. Du, J. Zelek, and J. Li, "Weather-aware autopilot: Domain generalization for point cloud semantic segmentation in diverse weather scenarios," *ISPRS*, vol. 218, pp. 204–219, 2024.

[28] P. He, L. Jiao, L. Li, X. Liu, F. Liu, W. Ma, S. Yang, and R. Shang, "Domain generalization-aware uncertainty introspective learning for 3d point clouds segmentation," in *ACMMM*, 2024, pp. 651–660.

[29] J. Park, K. Kim, and H. Shim, "Rethinking data augmentation for robust lidar semantic segmentation in adverse weather," in *ECCV*, 2024, pp. 320–336.

[30] X. Huang and S. Belongie, "Arbitrary style transfer in real-time with adaptive instance normalization," in *ICCV*, 2017, pp. 1501–1510.

[31] D. Ren, S. Wang, Z. Zhang, W. Yang, M. Ren, and H. Zhang, "Unsupervised cross domain semantic segmentation with mutual refinement and information distillation," *Neurocomputing*, vol. 586, p. 127641, 2024.

[32] J. Liu, Y. Chen, H. Liu, H. Zhang, and Y. Zhang, "From less to more: Progressive generalized zero-shot detection with curriculum learning," *TITS*, vol. 23, no. 10, pp. 19 016–19 029, 2022.

[33] D. Ren, M. Li, S. Wang, M. Ren, and H. Zhang, "Safenet: Semantic-aware feature enhancement network for unsupervised cross-domain road scene segmentation," *Image and Vision Computing*, vol. 152, p. 105318, 2024.

[34] A. Geiger, P. Lenz, and R. Urtasun, "Are we ready for autonomous driving? the kitti vision benchmark suite," in *CVPR*, 2012, pp. 3354–3361.

[35] E. Tzeng, J. Hoffman, K. Saenko, and T. Darrell, "Adversarial discriminative domain adaptation," in *CVPR*, 2017, pp. 7167–7176.

[36] T.-H. Vu, H. Jain, M. Bucher, M. Cord, and P. Pérez, "Advent: Adversarial entropy minimization for domain adaptation in semantic segmentation," in *CVPR*, 2019, pp. 2517–2526.

[37] Y. Zou, Z. Yu, X. Liu, B. Kumar, and J. Wang, "Confidence regularized self-training," in *ICCV*, 2019, pp. 5982–5991.